



# Stream metabolism increases with drainage area and peaks asynchronously across a stream network

Francine H. Mejia<sup>1,2,3</sup> · Alexander K. Fremier<sup>2</sup> · Joseph R. Benjamin<sup>4</sup> · J. Ryan Bellmore<sup>5</sup> · Adrienne Z. Grimm<sup>1,2,6</sup> · Grace A. Watson<sup>7</sup> · Michael Newsom<sup>8</sup>

Received: 1 April 2018 / Accepted: 1 December 2018

© This is a U.S. government work and not under copyright protection in the U.S.; foreign copyright protection may apply 2018

## Abstract

Quantifying the spatial and temporal dynamics of stream metabolism across stream networks is key to understanding carbon cycling and stream food web ecology. To better understand intra-annual temporal patterns of gross primary production (GPP) and ecosystem respiration (ER) and their variability across space, we continuously measured dissolved oxygen and modeled stream metabolism for an entire year at ten sites across a temperate river network in Washington State, USA. We expected GPP and ER to increase with stream size and peak during summer and autumn months due to warmer temperatures and higher light availability. We found that GPP and ER increased with drainage area and that only four sites adhered to our expectations of summer peaks in GPP and autumn peaks in ER while the rest either peaked in winter, spring or remained relatively constant. Our results suggest the spatial arrangement and temporal patterns of discharge, temperature, light and nutrients within watersheds may result in asynchronies in GPP and ER, despite similar regional climatic conditions. These findings shed light on how temporal dynamics of stream metabolism can shift across a river network, which likely influence the dynamics of carbon cycling and stream food webs at larger scales.

**Keywords** Asynchrony · GPP · ER · River networks · Production · Respiration · Stream metabolism

## Introduction

Ecosystem metabolism is an integrated functional measurement of the formation and utilization of organic matter by all the organisms within an ecosystem. The dominant pathway of metabolism includes production of organic matter via photosynthesis (gross primary production, GPP) and consumption of organic matter by both autotrophs and heterotrophs (ecosystem respiration, ER).

The primary drivers of stream metabolism are light availability, temperature, nutrients, autotrophic biomass, organic matter supply, and hydrology (Bernot et al. 2010). Each driver has a spatial and temporal pattern of its own, which, along with the transfer of energy and materials through a watershed, leads to a dynamic landscape of energy production and consumption (Uehlinger 2006; Roberts et al. 2007; Bernot et al. 2010; Tank et al. 2010). Peaks in metabolism are expected when energy inputs (light or leaf litter) and temperature are elevated and disturbance events (high flows) are absent. In montane regions, for example, snowmelt flows peak in the spring and can reduce GPP and ER (Uehlinger and Naegeli 1998) due to high turbidity and bed scour, but as

✉ Francine H. Mejia  
fmejia@usgs.gov

<sup>1</sup> Department of Fish and Wildlife Sciences, College of Natural Resources, University of Idaho, Moscow, ID 83844, USA

<sup>2</sup> School of the Environment, Washington State University, Pullman, WA 99164, USA

<sup>3</sup> U.S. Geological Survey, Forest and Rangeland Ecosystem Science Center, Cascadia Field Station, School of Environmental and Forest Sciences, University of Washington, Box 352100, Seattle, WA 98195, USA

<sup>4</sup> U.S. Geological Survey, Forest and Rangeland Ecosystem Science Center, Boise, ID 83702, USA

<sup>5</sup> USDA Forest Service, Pacific Northwest Research Station, Juneau, AK 99801, USA

<sup>6</sup> GeoSystems Analysis, Inc, 1412 13th St., Suite 200, Hood River, OR 97031, USA

<sup>7</sup> Methow Salmon Recovery Foundation, Twisp, WA 98856, USA

<sup>8</sup> Geophilia Consulting, 1015 NE Dean Street, Portland, OR 97211, USA

flows decline, elevated light and temperature can stimulate in stream metabolism.

Seasonal patterns of metabolism, however, may be more controlled by local drivers rather than regional (Valett et al. 2008; Ogdahl et al. 2010; Dodds et al. 2018). Valett et al. (2008) suggested that seasonal patterns of stream metabolism differ along a gradient depending on the relative influences of local resource subsidies and in-stream autochthonous resources. For example, although the amount of incoming sunlight may be relatively homogenous across a river network, the amount of light available for primary production at the reach-scale is a function of local hillslope and vegetation shading (Greenwood and Rosemond 2005; Julian et al. 2008; Finlay et al. 2011). Consequently, conditions at the local scale could result in asynchronous patterns in GPP and ER within river networks.

In streams, ecosystem metabolism varies spatially across a network and temporally throughout the year and reflects environmental conditions across a range of spatial and temporal scales (e.g. local to regional, immediate to annual) (Roberts et al. 2007; Ogdahl et al. 2010; Yates et al. 2013). A number of studies have examined spatial (e.g., Finlay 2011; Yates et al. 2013; Dodds et al. 2018) and temporal variation (e.g., Uehlinger and Naegeli 1998; Roberts et al. 2007; Beaulieu et al. 2013) in stream metabolism, but seldom simultaneously (but see, Young and Huryn 1996; Griffiths et al. 2013; Venkiteswaran et al. 2015), continuously (but see, Izaguirre et al. 2008), and rarely in winter (but see, Hart 2013; Val et al. 2016; Ulseth et al. 2018). There is need for a more continuous description of the spatial and temporal arrangement of stream metabolism because GPP and ER control basal resource dynamics and in turn the structure and function of river food webs (Bernhardt et al. 2017, Saunders et al. 2018).

In this paper, to better understand intra-annual temporal patterns of GPP and ER and their variability across space, we continuously measured dissolved oxygen and modeled stream metabolism for an entire year at ten sites across a river network. We asked the following questions: (1) what are the seasonal patterns of GPP and ER and how do they vary across the river network? And, (2) what environmental factors control spatial and temporal dynamics? We expected that GPP and ER would generally increase with stream size because of greater light availability and water temperature in a wider river segment that occupy lower elevations. We also expected that GPP and ER would peak in the summer/autumn due to low flows, warmer water temperatures, and elevated resource availability (light and organic matter). However, we anticipated potential variability in GPP and ER at finer temporal scales due to variation in local environmental conditions across the river network.

## Methods

### Study area

The Methow River is an alluvial tributary to the Columbia River in north central Washington State (USA). The Methow River catchment area is 4462 km<sup>2</sup>, ranging in elevations from 2700 m in the Cascade Mountains to 240 m at the confluence with the Columbia River. The basin has a snowmelt driven hydrology with high altitude areas on the western side of the basin receiving approximately 2000 mm of precipitation annually (mainly as snow) and areas in the lower river valley receiving 300 mm (Konrad 2006). The river has a largely unaltered flow regime with high flows during May–June, and low flows during August–March. Flows during the study were representative of flows within the historic record at USGS gage 12448500 (Methow River at Winthrop), except for flows in September and October 2013 that were more than twice as high as mean average flows (1912–2014). The riparian corridors are generally intact and dominated by Douglas-fir (*Pseudotsuga menziesii*) and pine (*Pinus* spp.) in higher elevation reaches, and black cottonwood (*Populus trichocarpa*), and grey alder (*Alnus incana*) in lower areas (Zuckerman 2015).

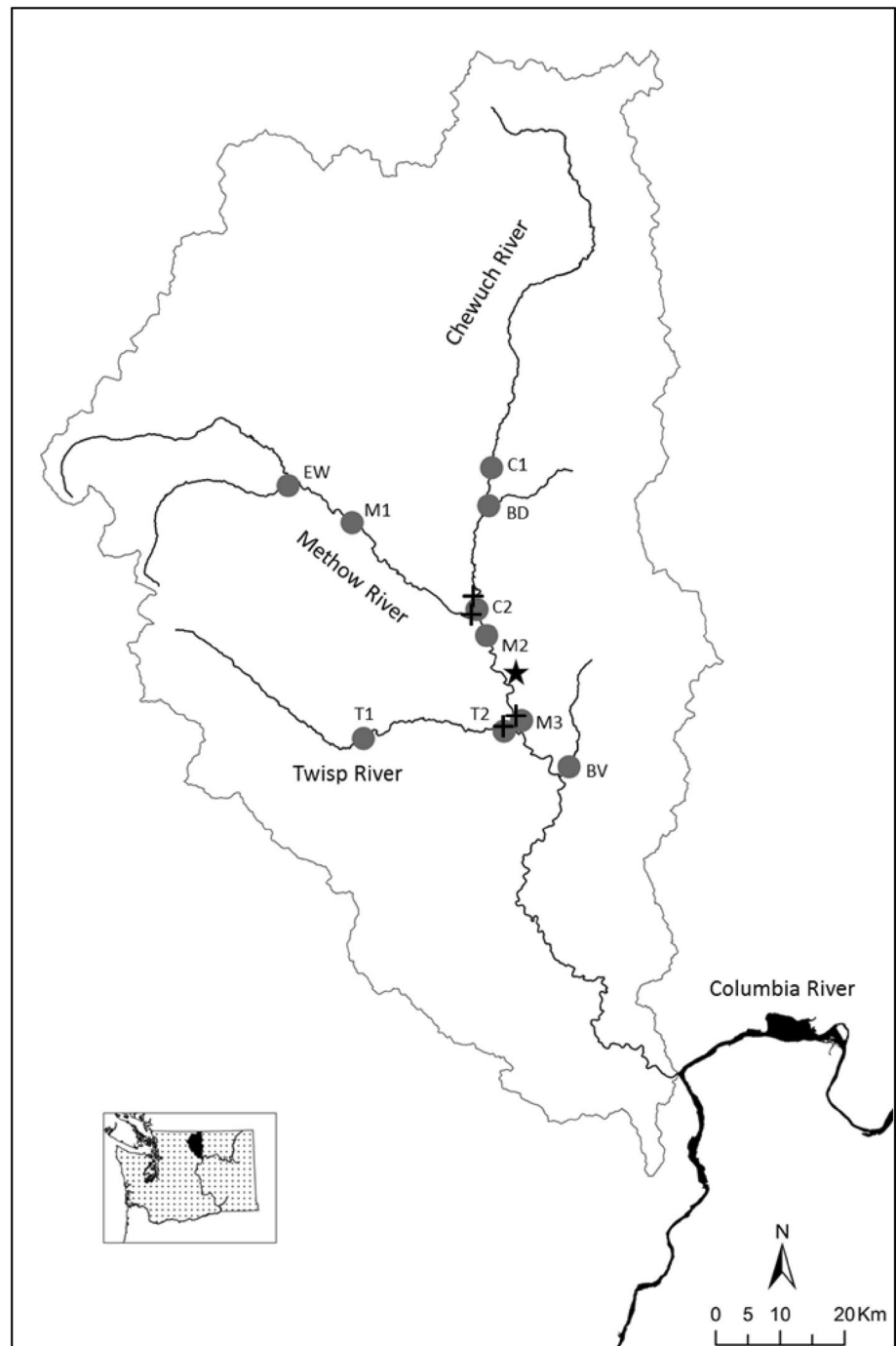
### Study design

To examine the spatial and temporal patterns in stream metabolism across a stream network, we continuously measured dissolved oxygen (DO) from June 2013 to May 2014 at 10 sites (Fig. 1) selected from a list of 52 intensively monitored sites that were part of the Columbia River Habitat Monitoring Program (CHaMP; <http://www.champmonitoring.org>). Sites were selected to represent the range of natural variability in environmental factors that might influence stream metabolism (Table 1). Sites ranged from small streams in confined valleys to relatively large streams in unconfined floodplains. Site selection was also constrained to those that had access in winter, landowner permission, and lacked nearby irrigation drains and major groundwater or tributary inputs.

### Stream metabolism measures

At each site, we measured stream metabolism via the open channel, single-station, diel O<sub>2</sub> method (Odum 1956). The single-station method generally integrates anywhere from 1 to 20 km up-stream from the point where dissolved oxygen is recorded. In our study, the reaches likely integrated between 200 m in the smaller creeks to near a kilometer in larger main-stem sections of the Methow River (Grace and Imberger 2006). These distances are corroborated by

**Fig. 1** Map of the Methow River basin. The ten sites, main tributaries and Columbia River are identified by name. The inset indicates the location of the Methow River in Washington State, USA. Black star represents location of PAR sensor. Black crosses represent USGS stream gages at Twisp River, Methow River near Twisp and Methow River near Winthrop, and Chewuch River



a previous metabolism study in the Methow River where single-station distances were calculated to be between 500 and 1700 m. We recorded dissolved oxygen concentrations and water temperature every 10 min from June 2013 to May 2014 in the channel thalweg with an YSI sonde (Yellow Springs, Ohio, USA) outfitted with an optical oxygen probe and a temperature probe.

We re-calibrated the sondes in the field approximately every 2 weeks in a bucket of air-saturated water using an air

pump and air stone (Hall et al. 2016). We later corrected our DO readings for drift that occurred between calibration periods (Grace and Imberger 2006). Gaps in data occurred when sondes were removed for high flows, ice-over conditions, or sensor malfunction and we did not estimate metabolism for these days.

We used the 3-parameter version of the Bayesian Single-station Estimation (BASE) program (light saturation and temperature dependence coefficients fixed) to estimate

**Table 1** Biological, chemical and physical characteristics for sites sampled in the Methow River basin. Standard deviation is in parentheses

| Site | GPP<br>gO <sub>2</sub> m <sup>-2</sup> day <sup>-1</sup> | ER          | K <sub>600</sub><br>day <sup>-1</sup> | Chl-a<br>mg m <sup>-2</sup> | AFDM<br>gm <sup>-2</sup> | PAR<br>μmol m <sup>-2</sup> s <sup>-1</sup> | Temp<br>°C | DIN<br>mg l <sup>-1</sup> | SRP<br>mg l <sup>-1</sup> | DA<br>km <sup>2</sup> | RBS<br>Vc/Vb | Q<br>m <sup>3</sup> s <sup>-1</sup> |
|------|--|-------------|---------------------------------------|-----------------------------|--------------------------|---|------------|---------------------------|---------------------------|-----------------------|--------------|-------------------------------------|
| BD   | 0.02 (0.01)  | 0.22 (0.27) | 16.2 (13.7)                           | 13.7 (2.7)                  | 6.07 (1.10)              | 83 (100)                                    | 6.0 (5.9)  | 0.04 (0.02)               | 0.008 (0.0040)            | 128                   | 6.62         | 0.38 (0.17)                         |
| EW   | 0.04 (0.06)  | 0.21 (0.19) | 13.2 (6.3)                            | 9.2 (3.9)                   | 4.02 (1.20)              | 199 (142)                                   | 7.3 (4.4)  | 0.05 (0.02)               | 0.001 (0.0002)            | 129                   | 4.37         | 2.17 (1.06)                         |
| BV   | 0.26 (0.21)  | 0.66 (0.49) | 12.8 (5.5)                            | 100.7 (67.9)                | 15.57 (8.35)             | 242 (141)                                   | 6.7 (5.7)  | 0.30 (0.08)               | 0.010 (0.0029)            | 179                   | 1.69         | 0.47 (0.36)                         |
| TI   | 0.08 (0.06)  | 1.17 (0.36) | 5.4 (1.8)                             | 5.2 (2.4)                   | 3.45 (1.12)              | 195 (162)                                   | 6.1 (4.4)  | 0.07 (0.03)               | 0.001 (0.0007)            | 211                   | 2.97         | 1.94 (1.90)                         |
| T2   | 0.51 (0.32)  | 1.08 (0.43) | 10.6 (3.5)                            | 31.8 (16.2)                 | 10.17 (2.47)             | 264 (160)                                   | 10.3 (5.4) | 0.08 (0.02)               | 0.001 (0.0003)            | 394                   | 0.86         | 2.39 (0.91)                         |
| C1   | 0.40 (0.16)  | 1.03 (0.32) | 6.5 (1.9)                             | 23.1 (9.8)                  | 9.32 (2.02)              | 176 (133)                                   | 5.7 (5.7)  | 0.04 (0.02)               | 0.003 (0.0026)            | 536                   | 3.02         | 2.14 (2.52)                         |
| M1   | 0.35 (0.24)  | 1.44 (0.67) | 5.8 (1.8)                             | 10.2 (4.6)                  | 5.43 (2.04)              | 284 (227)                                   | 7.6 (3.6)  | 0.05 (0.02)               | 0.002 (0.0005)            | 666                   | 3.62         | 6.30 (4.89)                         |
| C2   | 0.39 (0.15)  | 0.94 (0.44) | 9.3 (4.0)                             | 28.3 (12.4)                 | 11.91 (6.93)             | 203 (148)                                   | 8.4 (5.5)  | 0.05 (0.02)               | 0.002 (0.0005)            | 843                   | 2.74         | 2.55 (1.21)                         |
| M2   | 2.14 (0.89)  | 2.74 (1.02) | 8.5 (2.1)                             | 42.3 (31.3)                 | 15.33 (7.64)             | 300 (183)                                   | 7.6 (4.6)  | 0.10 (0.03)               | 0.002 (0.0007)            | 1669                  | 1.02         | 13.33 (7.46)                        |
| M3   | 2.53 (0.61)  | 3.03 (1.09) | 6.6 (1.1)                             | 44.1 (22.7)                 | 14.69 (6.61)             | 204 (137)                                   | 6.8 (4.8)  | 0.20 (0.04)               | 0.002 (0.0011)            | 1722                  | 1.58         | 10.35 (5.50)                        |

GPP gross primary production, ER ecosystem respiration, K<sub>600</sub> normalized reaeration coefficient with Schmidt number of 600, Chl-a chlorophyll-a, AFDM ash free dry biomass, PAR photosynthetically active radiation, Temp temperature, DIN dissolved inorganic nitrogen, SRP soluble reactive phosphorus, DA drainage area, RBS relative bed stability, Q discharge

stream metabolism from the diel DO curves (Grace et al. 2015). The BASE program estimates single-station whole stream metabolism using Bayesian statistics. We reconstructed the diurnal cycle of DO concentration to estimate daily GPP and ER through 8000 iterations, after allowing the model to reach equilibrium (i.e., burn-in of 2000 iterations), using a Markov Chain Monte Carlo (MCMC) method to estimate values of each parameter.

The batch mode of the BASE program fits observed oxygen data for many days by selecting best fit parameter values for reaeration, ER and GPP, and then provides visual and statistical measures of “goodness-of-fit”. This dynamic modeling approach allows for the simultaneous estimation of reaeration (K), GPP and ER and provides a way to mechanistically characterize GPP, ER and K in larger systems (Demars et al. 2015; Song et al. 2016). We selected the BASE program because of its capability to indirectly estimate reaeration. This was necessary because most of the reaches were large enough that air–water gas exchange measurements would be logistically challenging and difficult to completely mix across the reach.

We evaluated daily model fit using: (1) the correlation coefficient (R<sup>2</sup>) between the modeled and measured DO data, (2) a posterior predictive check (PPC) that measures the overall fit based on the 8,000 Markov chain Monte Carlo iterations used to estimate GPP and ER (Grace et al. 2015) and (3) visual assessment of K. We only used daily models with an R<sup>2</sup> ≥ 0.6 and a PPC between 0.1 and 0.9. The mean R<sup>2</sup> for all daily models was 0.92 (±0.08 SD) and mean PPC = 0.63 (±0.13 SD). After applying this set of criteria for model fitting, we deemed 1373 days across the calendar year and ten sites as good fits (56% of the total days modeled). Grace et al. (2015) found that BASE successfully converged and fitted 78% of the DO diel curves included in their evaluation of their model. Our lower percentage may be attributed to cold water temperatures, low productivity and high turbulence (M.R. Grace, Monash University, Melbourne, Australia, Personal Communication). We discarded the poorly fit diel curves and did not include incomplete days or periods where DO probes malfunctioned. Because we solved for K, GPP and ER simultaneously there was a risk of overfitting the model (Demars et al. 2015; Hall and Hotchkiss 2017) so we further evaluated the quality of our K estimates after we discarded the poorly fit diel curves. We converted our K estimates to K<sub>600</sub> to compare our estimates to those published in the literature (Hall and Hotchkiss 2017) and determined that they were within the range of values provided by Hall et al. (2012), Griffiths et al. (2013), and Hall et al. (2016). In addition, we determined that half of the sites had K<sub>600</sub> variability equal or less than two standard deviations and that variability was larger for the smaller streams. K<sub>600</sub> variability was close to or exceeded 50% for smaller streams indicating high uncertainty in K<sub>600</sub> estimates

(Table 1). We plotted  $K_{600}$  against  $\log Q$  and found that most sites were not correlated (Fig. 2). However, we observed a strong relationship between  $K_{600}$  and river slope ( $R^2=0.73$ ,  $p=0.001$ ) indicating that site geomorphology may have a greater influence on  $K_{600}$  than discharge. We also plotted  $K_{600}$  against ER and found that most sites were also not correlated.

We converted GPP and ER estimates from per volume rates ( $\text{mgO}_2 \text{ l}^{-1} \text{ day}^{-1}$ ) to areal rates ( $\text{g O}_2 \text{ m}^{-2} \text{ day}^{-1}$ ) by dividing by the mean stream depth. Stream depth was measured monthly along a transect representative of the reach at each site. Continuous depth estimates were then calculated by generating equations that related discharge and depth as a power function from either the data collected in the transects measured monthly or at the USGS gages (Table 2).

In addition to DO data, the BASE program requires inputs of barometric pressure, water temperature, photosynthetic active radiation (PAR; described below), and salinity to estimate metabolism. We obtained barometric pressure data (in Hg) recorded from Chief Joseph Dam Washington Agrimet Cooperative Agricultural weather network station, which we corrected for the local altitude at each site. We assumed salinity to be 0 because of the low electric conductance in the Methow River (maximum electrical conductance  $< 500 \mu\text{S cm}^{-1}$ ) (following Grace and Imberger 2006).

**Table 2** Exponents and coefficients for the power function relationship between depth (m) and discharge ( $\text{m}^3 \text{ s}^{-1}$ ) for sites sampled in the Methow River basin

| Site | Exponent | Coefficient | $R^2$ |
|------|----------|-------------|-------|
| BD   | 0.2526   | 0.2912      | 0.87  |
| EW   | 0.4125   | 0.207       | 0.93  |
| BV   | 0.5105   | 0.6081      | 0.63  |
| T1   | 0.4281   | 0.1963      | 0.99  |
| T2   | 0.3222   | 0.2411      | 0.89  |
| C1   | 0.2025   | 0.2661      | 0.65  |
| M1   | 0.2778   | 0.2193      | 0.94  |
| C2   | 0.4242   | 0.2149      | 0.91  |
| M2   | 0.4107   | 0.1838      | 0.97  |
| M3   | 0.3439   | 0.2519      | 0.87  |

### Periphyton, nutrient and physical measurements

To explore which environmental factors control stream metabolism at each site, we measured periphyton biomass, nutrient concentration, PAR, discharge, drainage area, and relative bed stability (RBS). At each site, we took monthly samples of periphyton from five randomly selected rocks in the active channel at 10 m intervals upstream of the dissolved oxygen sensors. We removed all periphyton from each rock, filtered the slurry, and froze the slurry for later lab analysis for Chlorophyll-*a* (Chl-*a*,  $\text{mg m}^{-2}$ ) and

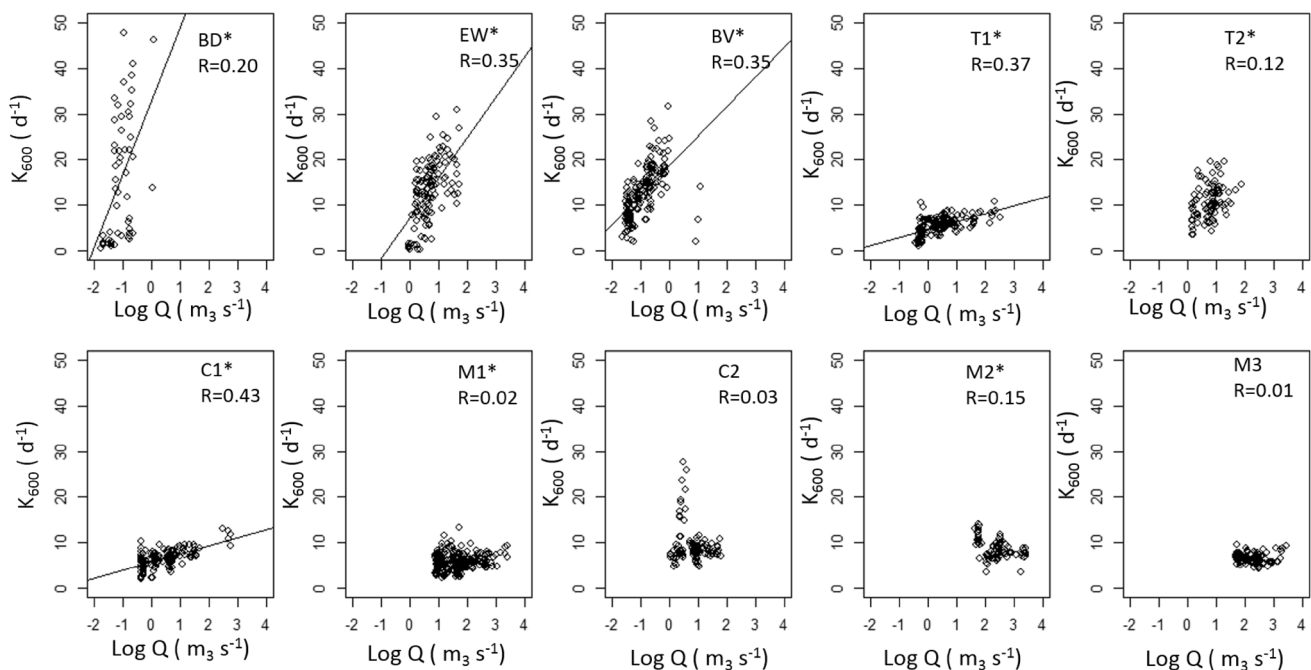


**Fig. 2** Relationship between discharge ( $\log Q$ ,  $\text{m}^3 \text{ s}^{-1}$ ) and gas exchange scaled to a Schmidt number of 600,  $K_{600} \text{ day}^{-1}$  for all sites ordered from smallest to largest drainage area. Asterisk represents a significant relationship

ash-free-dry-mass (AFDM,  $\text{g m}^{-2}$ ), following Standard Methods (APHA 2005). To quantify planar surface area, we traced the top surface of each rock on paper (Bergey and Getty 2006). Periphyton samples were taken monthly except on a few instances when flows were too high to access the streambed.

We collected one water sample at the downstream end of each site at monthly sampling intervals. Samples were immediately filtered ( $0.45 \mu\text{m}$ ), stored frozen and then analyzed using EPA standard methods (United States Environmental Protection Agency 1983) by IEH Analytical Laboratories (Seattle, Washington, USA) for ammonium ( $\text{NH}_4\text{-N}$ ), nitrate + nitrite ( $\text{NO}_3\text{-N}$ ,  $\text{NO}_2\text{-N}$ ), and soluble reactive phosphorus (SRP). In this study, we considered all three dissolved nitrogen species together as dissolved inorganic N (DIN). Detection limits for  $\text{NH}_4\text{-N}$ ,  $\text{NO}_3\text{-N}$ , and  $\text{NO}_2\text{-N}$  were  $0.01 \text{ mg L}^{-1}$  and for SRP was  $0.001 \text{ mg L}^{-1}$ .

We measured PAR with a PAR sensor and data logger (sensor model S-LIA-M003, data logger model H21-002, Onset Computer Corporation, Bourne, Massachusetts, USA) at a single, central, location free of aerial obstructions near Winthrop, WA. Readings were recorded every 30 min for the duration of the study to include in the metabolism model. This dataset represented the total incoming PAR available for primary production, which was adjusted for shading at each site by using a Solmetric Suneye 210 (Solmetric Corporation, Sebastopol, California, USA). At each site, we placed the Suneye near the center of the channel at three locations during August 2013 visits. The Suneye estimates the solar access percentage for every day of the year by taking into consideration sun paths. Solar access is the amount of site-specific solar insolation available given the shade-causing obstructions (e.g. tree canopy, topographic shading, structures) divided by the solar insolation if there were no shading. We multiplied each PAR measurement taken at the open site by the daily percentage solar access to estimate PAR experienced at each site.

We generated daily discharge ( $Q$ ,  $\text{m}^3 \text{ s}^{-1}$ ) estimates using the ratio of daily discharge to bankfull discharge from the closest USGS gages for each site. We multiplied the ratio by the bankfull discharge at the ungaged site (bankfull discharge was assumed to be the 2-year discharge as obtained from USGS StreamStats; Table 1) to create an adjusted dataset of mean daily discharge, as suggested by Leopold (1994) and Biedenharn et al. (2000). We obtained daily discharge from four nearby USGS gages (12448000, 12448500, 12448998, 12449500; Fig. 1). We estimated drainage area (Table 1) at each sampling location using StreamStats (USGS accessed August 7, 2015).

We calculated RBS as the ratio of the critical velocity required to move a particle to the predicted (bankfull) water velocity near the bed (Gordon et al. 2004). A ratio less than 1.0 represents the value at which particles are expected to

move. The streambed is considered highly stable if RBS values are greater than 1.0 at bankfull discharge (i.e., the 2-year discharge). The equation for critical velocity in SI units is  $V_c = 0.155 \sqrt{d}$  where  $d$  is the average particle diameter in mm. Bed velocity is 0.7 multiplied by the mean stream velocity ( $\text{m s}^{-1}$ ) at bankfull discharge.

## Statistical analyses

To test our expectation that GPP and ER would increase with stream size, we conducted Pearson correlations between metabolic rates (GPP and ER) and drainage area for each season. To evaluate our expectation that metabolism would peak in summer/autumn (with finer-scale temporal asynchronies), we plotted daily metabolism, and compared them across the network and visually inspected their respective peaks and valleys.

To infer potential drivers of metabolism, we used a linear mixed modeling approach (Zuur et al. 2009) with the nlme package for mixed effects modeling (R Development Core Team 2013). We conducted this analysis at both the watershed and reach scale to evaluate factors controlling metabolism both across and within sites. The explanatory variables for the models were AFDM, SRP, DIN, temperature (Temp), PAR and discharge ( $Q$ ) and the dependent variables were either GPP or ER. We also included GPP as an explanatory variable in the ER models. For the across site (watershed scale) analysis of GPP and ER, we included site and month as random effects to account for the repeated measures. For the within site (reach scale) analysis we included month as a random effect. We also used the variance structure varIdent to represent a constant variance function structure which is generally used to allow different variances according to the levels of a classification factor (e.g. month and site). varIdent was used when the Akaike Information Criterion (AIC) values determined this variance function structure was more appropriate than the unstructured variance function structure, as lower AIC values were associated with better model fits. We also accounted for the repeated measures and potential autocorrelation in both scales models (watershed and reach) by adding the autocorrelation structure corARMA. This correlation structure class represents an autocorrelation moving average correlation structure. We inspected deviations from the analysis assumptions using model diagnostic plots and accounted for heteroscedasticity by including variance functions (Pinheiro et al. 2017; Zuur et al. 2009). We did not find evidence of multicollinearity among explanatory variables (variance inflation factor  $< 3$ ); hence, all variables were included in the model selection procedure. We used the Akaike's Information Criterion corrected for small sample sizes (AICc) to select the best models and retained models that had a  $\Delta < 2$ . We also estimated  $R^2_{\text{GLMM}(m)}$ , marginal  $R^2$ , for fixed factors and  $R^2_{\text{GLMM}(c)}$  conditional  $R^2$  for both

fixed and random factors  $R^2_{GLMM(m)}$  using the R function 'r.squaredGLMM' from the package 'MuMIn' (Bartoń 2015). Before conducting the linear mixed modeling, we tested predictor variables for multicollinearity by comparing Pearson correlations between metabolism and predictor variables. We also tested normality with the Shapiro–Wilk test. All statistical analyses were performed in R (R Core Team 2013) and results were deemed significant if  $p < 0.05$ .

## Results

### What are the seasonal patterns of GPP and ER and how do they vary across the river network?

Temporal patterns of gross primary production and ecosystem respiration were strongly variable at different sites across the river network (Fig. 3). For GPP, the peaks and troughs in production were highly asynchronous and bimodal if the site remained ice-free during the winter. Some sites peaked in production in summer (BD, EW, C2, and T2), while others either had multiple peaks including winter peaks (C1, M1, M3, BV, and M2) or remained relatively consistent (T1). Summer peak sites either froze-over completely or partially from December to February (Fig. 3).

We found a similar result for ecosystem respiration (Fig. 3). Four sites exhibited generally higher ecosystem respiration in autumn (BD, EW, C2, and T2), where five exhibited more of a winter peak (BV, M1, C1, M2, and M3) and one remained relatively constant (T1).

Mean annual GPP and ER significantly increased with drainage area ( $r = 0.86$ ,  $p < 0.0001$ ;  $r = 0.75$ ,  $p < 0.0001$ , Table 1). On average, there was approximately two orders of magnitude increase in GPP ( $0.02$ – $2.53$  g O<sub>2</sub> m<sup>-2</sup> day<sup>-1</sup>, Table 1) and one order of magnitude increase in ER ( $0.22$ – $3.03$  g O<sub>2</sub> m<sup>-2</sup> day<sup>-1</sup>, Table 1) with increasing drainage area (Fig. 4). The positive correlations with drainage area was observed across seasons, although the relationship was weaker for ER during the spring (Fig. 4). Mean annual GPP and ER also were significantly correlated with Q (Pearson correlations of  $0.50$   $p < 0.0001$  and  $0.52$   $p = 0.002$ ), a variable related to stream size.

### How Do Environmental Conditions Change Through the Year?

Generally, decreasing daily discharge (Q) in the summer/autumn baseflows, coincided with decreasing light availability (PAR) and decreasing water temperatures across the basin (Figs. 3, 5). Discharge progressively decreased from July 2013 to April 2014 except for four smaller spates during the Summer/Autumn baseflow (two in August, one in September, and one in October). The number of days between

the last spate in October and the increasing flows in spring was approximately 180 days. We also determined that all sites are highly stable ( $RBS > 1$ ) at bankfull discharge. The RBS ratio ranged from 0.86 at T2 to 6.6 at BD. Most values were higher than 1.0, except for T2 and M2. Additionally, BD, EW C2 and T2 study reaches were 30–90% covered by ice in winter (Fig. 3).

Water temperature was highest in the spring and summer and lowest in the winter, for all sites (Fig. 5). Water temperatures near 0 were observed in most sites in winter, except at M1 where temperatures stayed above 2.5 °C. M1 also had the narrowest range of variation in water temperature (2.6–14.5 °C). In contrast, the greatest range of variation was observed in T2 (0.4–18.5 °C). Maximum PAR was observed in the summer in all sites with the lowest PAR site, BD receiving only half of that of the site with highest PAR observed, M1 (370 vs. 725) (Fig. 5). DIN concentrations increased in the winter for BV, C2 and M2 (Fig. 6) and was highest for BV. Soluble reactive phosphorus was generally very low but peaked in the summer for BV and C1 (Fig. 6). AFDM was highest for BV in winter and spring followed by M2 and M3 which also had AFDM peaks in the winter (Fig. 7). AFDM biomass was lowest in EW.

### Which environmental factors control spatial and temporal dynamics?

Based on the results of linear mixed models for individual stream sites, GPP was positively associated with water temperature in most sites (Table 3). GPP was also strongly negatively associated with discharge at half of the sites. This association with discharge when present, was stronger than the positive association with water temperature.

The linear mixed model for ecosystem respiration (ER) at individual sites confirmed that ER was highly correlated with GPP (Table 4). ER was positively associated with GPP in all sites. For the summer peak sites, ecosystem respiration was positively associated with discharge except for one stream.

Across the ten sites, both linear mixed models (GPP and ER) accounted for 36% and 56% of the fixed effects, respectively (Table 5). The linear mixed model for GPP showed that AFDM was the best predictor of differences in GPP ( $p < 0.0001$ ; Table 5). Soluble reactive phosphorus (SRP) and Q also significantly explained across site variability, although the percentages explained were low. For the across sites ER model, GPP was the best explanatory variable ( $p < 0.0001$ ). Discharge (Q), Temp and PAR explained a small portion of the across site variability as well.

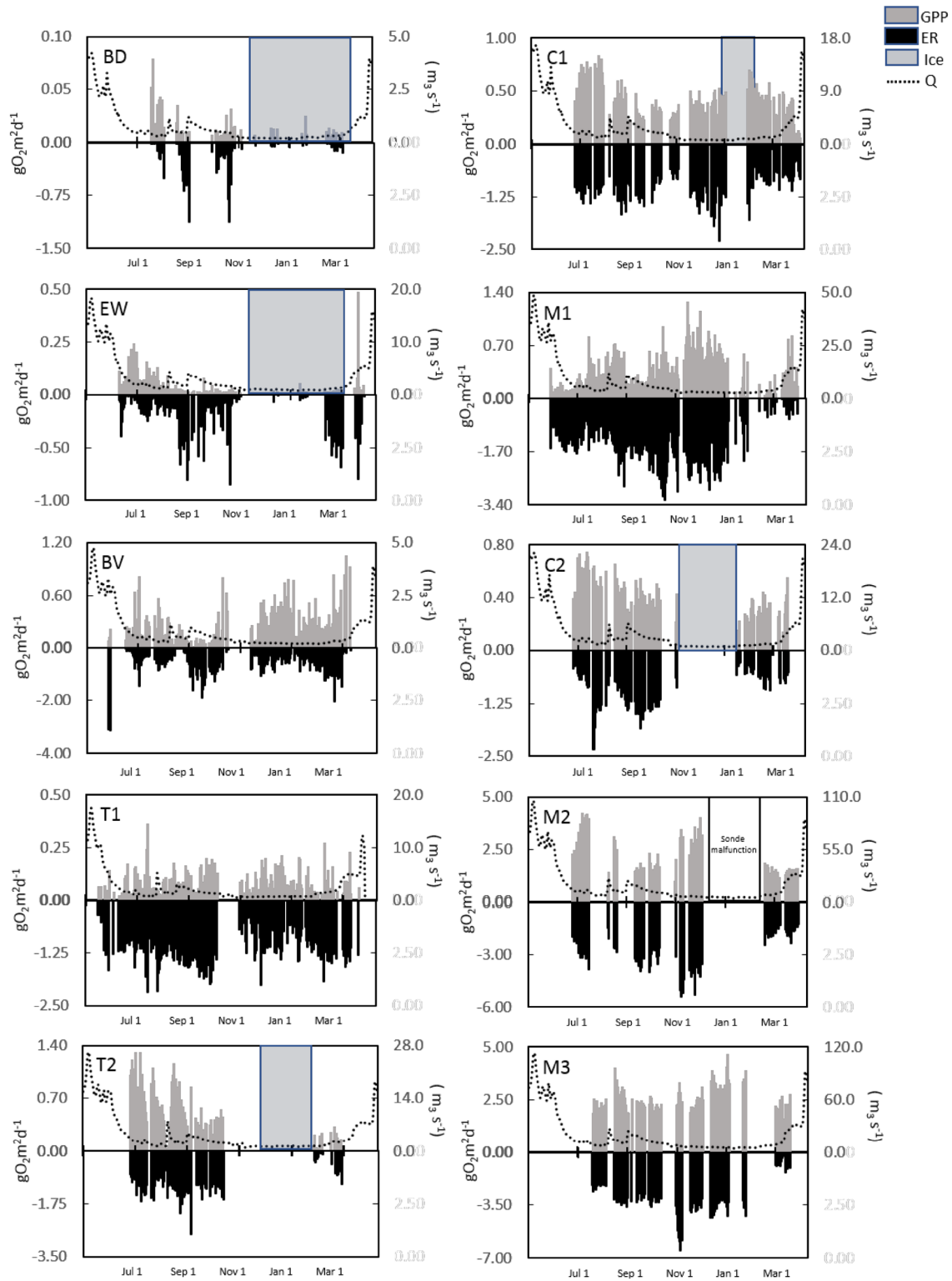


**Fig. 3** Daily gross primary production (GPP) and daily ecosystem respiration (ER) estimated across 10 sites within the Methow River network (sites were ordered from smallest to largest drainage area).

GPP and ER are in  $\text{g O}_2 \text{ m}^{-2} \text{ day}^{-1}$ . Sites, BD, EW, C2 and T2 were partially frozen from mid-December to mid-February. Dotted line represents daily discharge



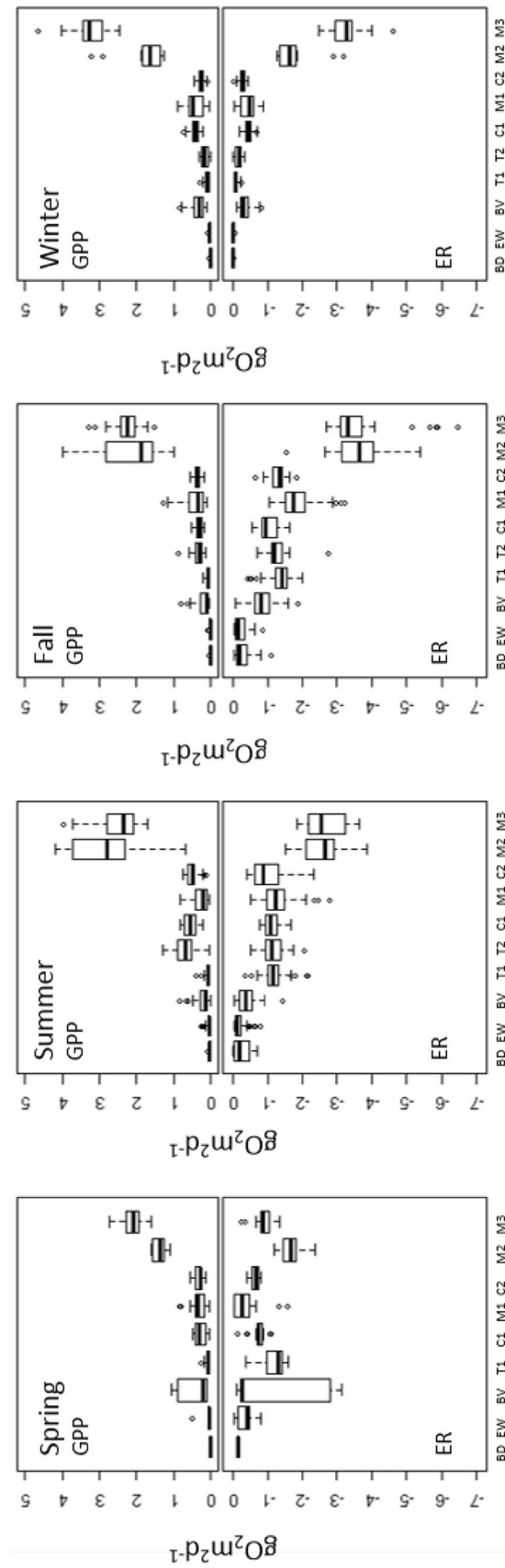
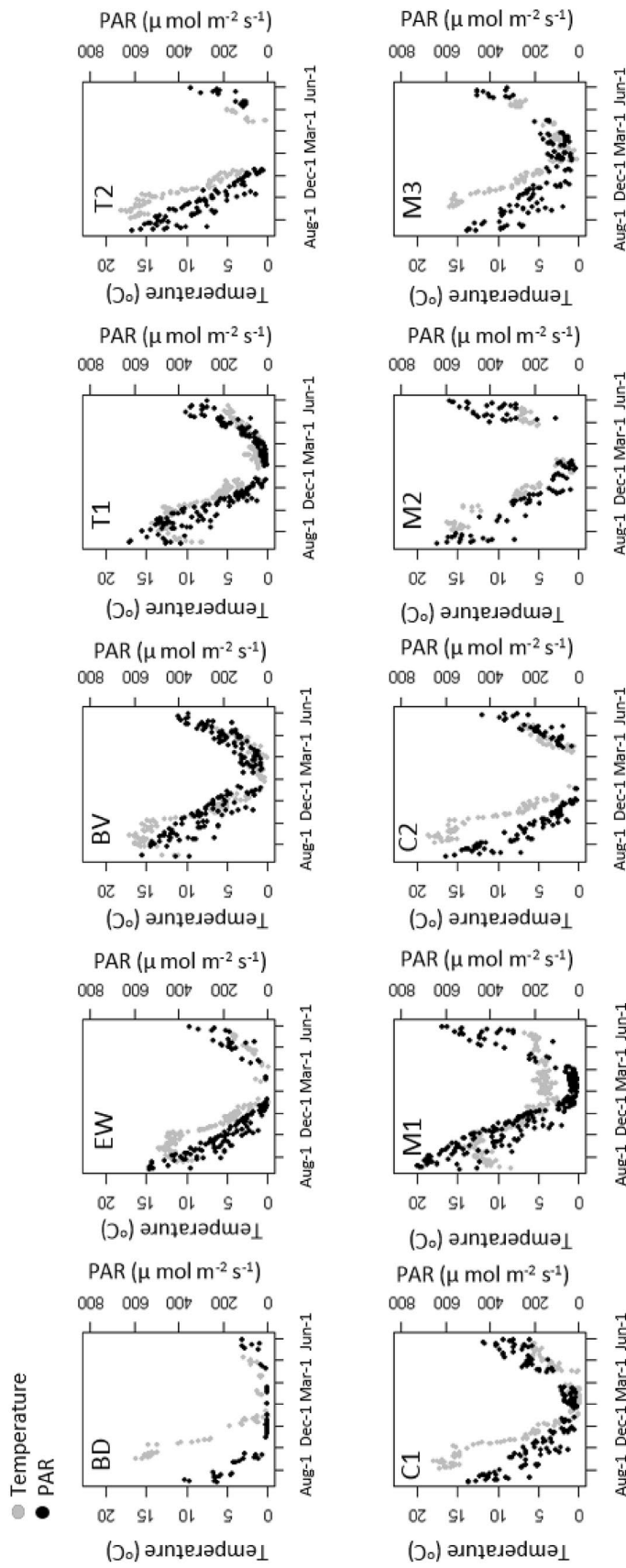
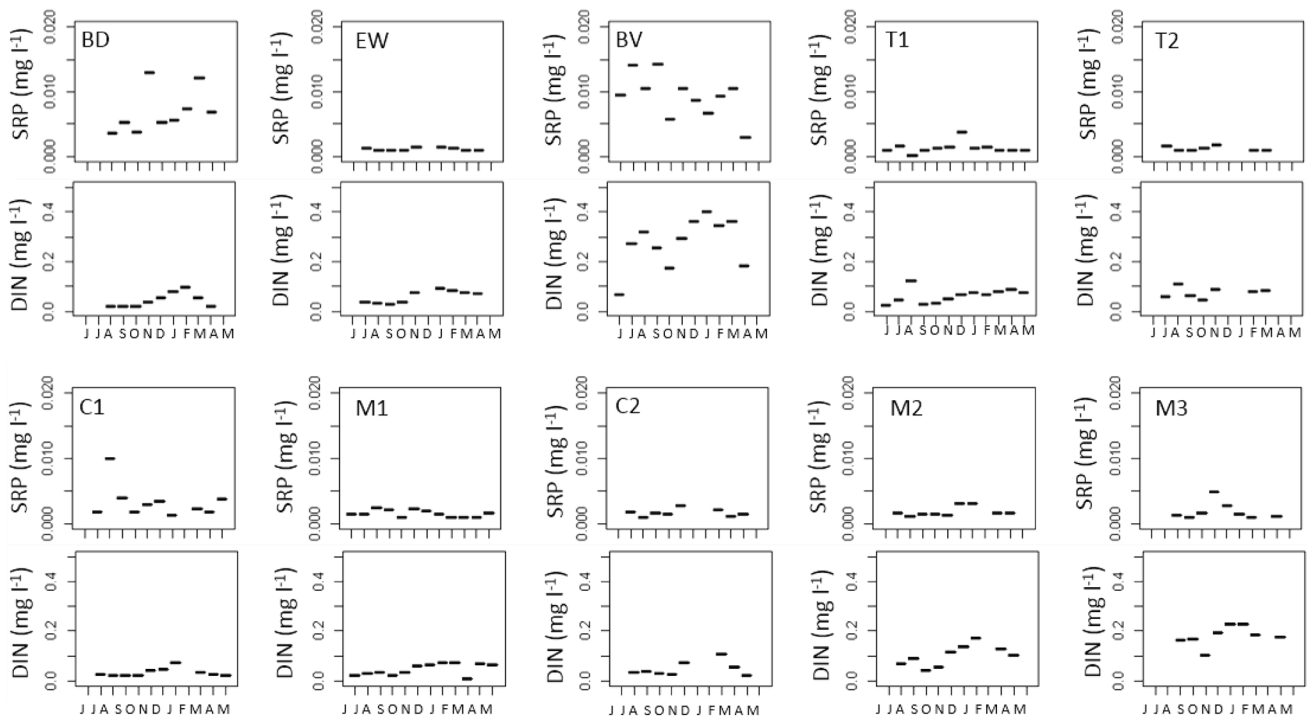


Fig. 4 Seasonal patterns of gross primary productivity (GPP) and ecosystem respiration, ER for spring, summer, fall, and winter. Sites were ordered from smallest to largest drainage area (left to right)

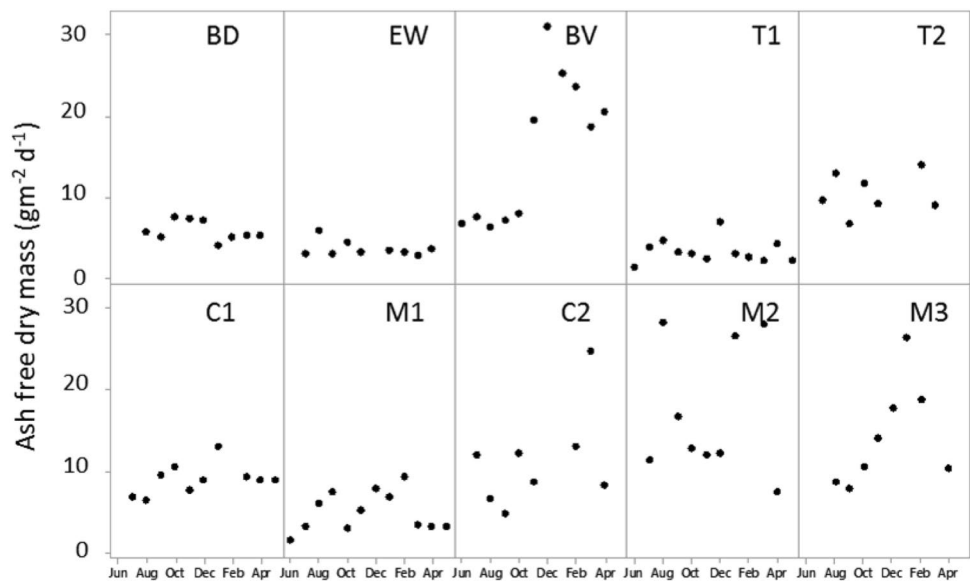


**Fig. 5** Daily temperature ( $^{\circ}\text{C}$ ) and photosynthetic active radiation (PAR,  $\mu\text{mol m}^{-2} \text{s}^{-1}$ ) for all 10 sites ordered from smallest to largest drainage area. Gray dots represent temperature. Black dots represent PAR



**Fig. 6** Dissolved inorganic nitrogen (DIN,  $\text{mg l}^{-1}$ ) and soluble reactive phosphorus (SRP,  $\text{mg l}^{-1}$ ) sampled monthly across 10 sites within the Methow River network (sites were ordered from smallest to largest drainage area)

**Fig. 7** Ash free dry mass (AFDM,  $\text{gm}^{-2} \text{day}^{-1}$ ) sampled monthly across 10 sites within the Methow River network (sites were ordered from smallest to largest drainage area)



### Discussion

Our findings illustrate that stream metabolism at sites within river networks can exhibit asynchronous temporal dynamics. However, on an annualized basis, metabolism followed an increase of GPP and ER with drainage area. These findings emphasize that inferences drawn from

“snap-shots” of metabolism (i.e., short duration studies; days to weeks) may strongly bias our understanding of the spatial arrangement of metabolism within watersheds, and points to the need for studies that incorporate both spatial and temporal dynamics.

We found distinct seasonal patterns in gross primary production (GPP) and ecosystem respiration (ER) across our ten

**Table 3** Coefficient estimates, standard errors, percent of the explained variance for fixed ( $R^2_m$ ) and random and fixed effects combined ( $R^2_c$ ) for gross primary production (GPP) models for each site (all dates combined)

|            | Value  | Std. error | DF  | t-value | p-value | $R^2_m$ | $R^2_c$ |
|------------|--------|------------|-----|---------|---------|---------|---------|
| BD         |        |            |     |         |         | 0.55    | 0.62    |
| Intercept  | -4.423 | 0.156      | 42  | -28.310 | 0.000   |         |         |
| Temp       | 0.055  | 0.010      | 42  | 5.730   | 0.000   |         |         |
| Log (Q)    | -0.334 | 0.112      | 42  | -2.990  | 0.005   |         |         |
| EW         |        |            |     |         |         | 0.43    | 0.51    |
| Intercept  | -2.128 | 0.894      | 126 | -2.381  | 0.019   |         |         |
| Temp       | 0.191  | 0.030      | 126 | 6.300   | 0.000   |         |         |
| Log (N)    | 0.919  | 0.337      | 7   | 2.729   | 0.029   |         |         |
| BV         |        |            |     |         |         | 0.48    | 0.56    |
| Intercept  | -7.914 | 0.995      | 158 | -7.953  | 0.000   |         |         |
| Log (AFDM) | 1.876  | 0.333      | 9   | 5.640   | 0.000   |         |         |
| Temp       | 0.164  | 0.030      | 158 | 5.401   | 0.000   |         |         |
| Log (Q)    | -0.368 | 0.192      | 158 | -1.917  | 0.057   |         |         |
| T1         |        |            |     |         |         | 0.20    | 0.36    |
| Intercept  | -0.925 | 0.298      | 177 | -3.102  | 0.002   |         |         |
| Temp       | 0.073  | 0.027      | 177 | 2.718   | 0.007   |         |         |
| Log (Q)    | 0.227  | 0.102      | 177 | 2.232   | 0.027   |         |         |
| Log (PAR)  | -0.467 | 0.075      | 177 | -6.209  | 0.000   |         |         |
| T2         |        |            |     |         |         | 0.56    | 0.56    |
| Intercept  | -1.591 | 0.166      | 95  | -9.587  | 0.000   |         |         |
| Temp       | 0.090  | 0.014      | 95  | 6.229   | 0.000   |         |         |
| C1         |        |            |     |         |         | 0.43    | 0.64    |
| Intercept  | 0.303  | 0.026      | 144 | 11.757  | 0.000   |         |         |
| Temp       | 0.011  | 0.003      | 144 | 3.743   | 0.000   |         |         |
| Log (Q)    | -0.099 | 0.018      | 144 | -5.390  | 0.000   |         |         |
| M1         |        |            |     |         |         | 0.18    | 0.48    |
| Intercept  | 0.521  | 0.080      | 217 | 6.533   | 0.000   |         |         |
| Temp       | 0.015  | 0.007      | 217 | 2.194   | 0.000   |         |         |
| Log (PAR)  | -0.069 | 0.016      | 217 | -4.403  | 0.000   |         |         |
| C2         |        |            |     |         |         | 0.49    | 0.64    |
| Intercept  | 0.247  | 0.037      | 108 | 6.656   | 0.000   |         |         |
| Log (Q)    | -0.072 | 0.028      | 108 | -2.608  | 0.010   |         |         |
| Temp       | 0.016  | 0.003      | 108 | 4.952   | 0.000   |         |         |
| M2         |        |            |     |         |         | 0.30    | 0.69    |
| Intercept  | 1.347  | 0.276      | 85  | 4.886   | 0.000   |         |         |
| Temp       | 0.041  | 0.017      | 85  | 2.397   | 0.019   |         |         |
| Log (Q)    | -0.400 | 0.111      | 85  | 3.590   | 0.000   |         |         |
| M3         |        |            |     |         |         | 0.30    | 0.53    |
| Intercept  | 1.027  | 0.095      | 109 | 10.814  | 0.000   |         |         |
| AFDM       | 0.015  | 0.006      | 6   | 2.523   | 0.000   |         |         |

sites. Four sites exhibited expected unimodal GPP dynamics with peaks in summer and troughs in winter. Five sites exhibited a surprising bimodal pattern with GPP peaks in both summer and winter and one site was relatively constant. The sites where GPP peaked in summer are the sites where ER peaked in autumn and those where GPP peaked in winter or had bimodal GPP peaks also exhibited ER winter peaks or bimodal peaks.

To our knowledge, only one other study has reported seasonal asynchrony for metabolism within a watershed (Ogdahl et al. 2010) and like in our study, metabolism increased downstream. Additionally, although few studies have measured GPP in winter, GPP peaks in winter and fall have been described for at least two studies in the northern hemisphere. In the Little Tennessee River, North Carolina, Hart (2013) observed late winter- early spring GPP peaks, which were most positively associated

**Table 4** Coefficient estimates, standard errors, percent of the explained variance for fixed effects ( $R^2_m$ ) and random and fixed effects combined ( $R^2_c$ ) for ecosystem respiration (ER) models for each site (all dates combined)

|            | Value  | Std. error | DF  | t-value | p-value | $R^2_m$ | $R^2_c$ |
|------------|--------|------------|-----|---------|---------|---------|---------|
| <b>BD</b>  |        |            |     |         |         | 0.43    | 0.43    |
| Intercept  | 0.540  | 0.077      | 42  | 7.038   | 0.000   |         |         |
| Log (GPP)  | -2.993 | 1.348      | 42  | -2.221  | 0.000   |         |         |
| Log (Q)    | 0.307  | 0.064      | 42  | 4.786   | 0.000   |         |         |
| <b>EW</b>  |        |            |     |         |         | 0.37    | 0.91    |
| Intercept  | 0.378  | 0.092      | 125 | 4.119   | 0.000   |         |         |
| Log (GPP)  | 0.613  | 0.176      | 125 | 3.480   | 0.001   |         |         |
| Temp       | -0.045 | 0.009      | 125 | -4.870  | 0.000   |         |         |
| <b>BV</b>  |        |            |     |         |         | 0.39    | 0.39    |
| Intercept  | 7.921  | 1.245      | 158 | 6.362   | 0.000   |         |         |
| Log (GPP)  | 0.461  | 0.053      | 158 | 8.767   | 0.000   |         |         |
| Log (AFDM) | -2.384 | 0.407      | 9   | -5.859  | 0.000   |         |         |
| Temp       | -0.238 | 0.033      | 158 | -7.209  | 0.000   |         |         |
| <b>T1</b>  |        |            |     |         |         | 0.20    | 0.90    |
| Intercept  | 0.915  | 0.087      | 179 | 10.493  | 0.000   |         |         |
| GPP        | 2.523  | 0.254      | 179 | 9.919   | 0.000   |         |         |
| <b>T2</b>  |        |            |     |         |         | 0.40    | 0.80    |
| Intercept  | 0.756  | 0.240      | 93  | 3.152   | 0.000   |         |         |
| GPP        | 1.270  | 0.081      | 93  | 15.590  | 0.000   |         |         |
| Temp       | -0.087 | 0.018      | 93  | -4.769  | 0.000   |         |         |
| log (Q)    | 0.486  | 0.09       | 93  | 5.376   | 0.000   |         |         |
| <b>C1</b>  |        |            |     |         |         | 0.55    | 0.90    |
| Intercept  | 0.518  | 0.074      | 145 | 6.977   | 0.000   |         |         |
| Log (GPP)  | 0.589  | 0.058      | 145 | 10.102  | 0.000   |         |         |
| <b>M1</b>  |        |            |     |         |         | 0.48    | 0.94    |
| Intercept  | 1.138  | 0.200      | 217 | 5.681   | 0.000   |         |         |
| GPP        | 1.731  | 0.126      | 217 | 13.791  | 0.000   |         |         |
| log (Q)    | -0.219 | 0.072      | 217 | -3.067  | 0.000   |         |         |
| <b>C2</b>  |        |            |     |         |         | 0.22    | 0.87    |
| Intercept  | 0.28   | 0.100      | 106 | 2.816   | 0.000   |         |         |
| Log (GPP)  | 0.991  | 0.097      | 106 | 10.213  | 0.000   |         |         |
| log (Q)    | 0.136  | 0.045      | 106 | 3.027   | 0.003   |         |         |
| Temp       | -0.023 | 0.008      | 106 | -2.980  | 0.000   |         |         |
| PAR        | 0.000  | 0.000      | 106 | 2.708   | 0.008   |         |         |
| <b>M2</b>  |        |            |     |         |         | 0.72    | 0.98    |
| Intercept  | 2.303  | 0.346      | 84  | 6.651   | 0.000   |         |         |
| GPP        | 0.840  | 0.054      | 84  | 15.474  | 0.000   |         |         |
| Temp       | -0.079 | 0.024      | 84  | -3.239  | 0.002   |         |         |
| Log (PAR)  | -0.156 | 0.019      | 84  | -8.032  | 0.000   |         |         |
| <b>M3</b>  |        |            |     |         |         | 0.70    | 0.80    |
| Intercept  | 1.889  | 0.369      | 107 | 5.119   | 0.000   |         |         |
| GPP        | 0.692  | 0.051      | 107 | 13.632  | 0.000   |         |         |
| Log (PAR)  | -0.150 | 0.054      | 107 | -2.788  | 0.000   |         |         |

with leaf abscission, and the amount of available light, and negatively associated with canopy cover. In the Kuparuk River, Alaska, GPP values were greater during the fall shoulder-season than those measured during the arctic summer and that increased nutrient availability, high chl-a

biomass and/or algal taxonomic composition were the main drivers for these peaks. (Kendrick and Huryn 2015).

The metabolic asynchrony observed in our study was contrary to our expectation that peaks would occur in the summer at all sites due to high temperatures, low flows and clear

**Table 5** Coefficient estimates, standard errors, percent of the explained variance for fixed effects ( $R^2_m$ ) and random and fixed effects combined ( $R^2_c$ ) for across sites gross primary production (GPP) and ecosystem respiration (ER) models

|                 | Value  | Std. error | DF   | t-value | p value | $R^2_m$ | $R^2_c$ |
|-----------------|--------|------------|------|---------|---------|---------|---------|
| GPP (all sites) |        |            |      |         |         | 0.36    | 0.86    |
| Intercept       | -5.675 | 0.730      | 1276 | -7.77   | 0.000   |         |         |
| Log (AFDM)      | 1.075  | 0.122      | 81   | 8.78    | 0.000   |         |         |
| Log (Q)         | -0.068 | 0.03       | 1276 | -2.291  | 0.022   |         |         |
| Log (Temp)      | 0.061  | 0.0135     | 1276 | 4.48    | 0.000   |         |         |
| Log (SRP)       | -0.412 | 0.101      | 81   | -4.067  | 0.000   |         |         |
| ER (all sites)  |        |            |      |         |         | 0.56    | 0.87    |
| Intercept       | 1.027  | 0.067      | 1274 | 15.32   | 0.000   |         |         |
| Log (GPP)       | 0.282  | 0.010      | 1274 | 27.55   | 0.000   |         |         |
| Log (Q)         | 0.076  | 0.014      | 1274 | 5.45    | 0.000   |         |         |
| Temp            | -0.034 | 0.004      | 1274 | -8.92   | 0.000   |         |         |
| Log (PAR)       | 0.02   | 0.007      | 1274 | 2.80    | 0.005   |         |         |

water. Furthermore, it suggests that stream metabolism can be controlled by local variation in driving variables despite overall similar watershed-scale drivers (e.g. mean temperature and light and their seasonality). Observed asynchrony in ecosystem production and consumption could, in turn, have implications for food web dynamics and organisms that occupy higher trophic levels (Moore et al. 2015). For example, mobile fish species as well as many aquatic-dependent terrestrial consumers (e.g., water birds) move between reaches to take advantage of differences in food availability that likely result from asynchronies in ecosystem metabolism (Schindler et al. 2015; Walter et al. 2017).

Timing of peaks in GPP across the ten sites were likely due to different local environmental conditions. Our observational study does not allow us to make definitive conclusions about specific drivers, so we discuss some observations from our analysis. Sites where GPP peaked in the winter were generally larger and more productive sites located lower in the watershed, compared to summer peaking sites. Sites with winter peaks also lacked seasonal disturbance (i.e., high discharge events, ice formation), which could have allowed periphyton biomass to buildup until high flow events in the spring. The number of days between the last spate that took place in October and the beginning of the spring flows in early April was approximately 180 days. Larger river sites have also been shown to have higher nitrogen recycling (Ensign and Doyle 2006), which might also have stimulated GPP in the cooler months. In contrast, all the summer peak sites, were either partly or entirely frozen over during the winter month, which can substantially limit the amount of light reaching the benthos to fuel GPP (Wetzel 2001). Summer peak sites may have potential simultaneous or serial colimitations by light/temperature and nutrients. In summer peak sites, GPP was positively associated with water temperature, but not PAR. However, PAR also likely mediated stream temperatures.

In most sites, DIN and SRP concentrations were very low and characteristic of oligotrophic conditions (Minshall et al. 2014). Surprisingly, individual sites were not consistently associated with nutrients. This could be because nutrient samples were only taken once a month and these samples could have been taken at times where nutrients in the water column were uncharacteristically high or low. Future studies should consider more frequent sampling of DIN and SRP. Alternatively, measurements of nutrient uptake may be better indicator of biological activity at the time of measurement (Hoellein et al. 2013).

Ecosystem respiration (ER) peaks for both groups (autumn and winter) were associated with GPP. Overall, GPP and ER were highly coupled during base flow conditions (October through March), when labile autochthonous carbon is likely to be an important source of organic carbon fueling ER (Townsend et al. 2011). The positive associations of ER with GPP may suggest high autotrophic respiration where high rates of GPP yield higher ER because of the combined respiration of autotrophs and heterotrophic organisms present in the biofilms (Hall et al. 2016).

Despite observed temporal asynchronies among sites, spatial patterns of GPP and ER corresponded with our expectation of increased metabolism with drainage area. On average, GPP increased two orders of magnitude and ER increased one order of magnitude with increasing drainage area. This pattern corresponded to that found in other studies (Lamberti and Steinman 1997; Finlay 2011). Although the mechanism for this downstream increase was not entirely clear from our analyses, our results of relative bed stability showed most sites in the watershed are rather stable so these stable downstream sites that did not ice-over were able to accumulate greater biofilm standing stocks, which supported greater GPP and ER. It is also likely that light availability, temperature and nutrients were also responsible for observed downstream increases in GPP and ER (Lamberti

and Steinman 1997; Finlay 2011). Individually, however, these variables were only weakly correlated with the downstream increase in metabolic rates.

Our main purpose was to explore the relative temporal and spatial patterns of ecosystem metabolism among the ten sites in the Methow River watershed, and how local and network scale factors may be driving these patterns. However, we acknowledge that we may be under- or over-estimating rates of GPP and ER in some of the sites. This may be especially true in the smaller streams where reaeration was highest (McCutchan et al. 1998; Aristegi et al. 2009). Under these circumstances, a benthic chamber method may be more appropriate for estimations (Grace and Imberger 2006) or estimating gas exchange using a tracer addition (Demars et al. 2015; Hall and Hotchkiss 2017). Furthermore, when GPP and ER estimates are low, our ability to estimate stream metabolism may not be precise enough to accurately assess temporal and spatial changes. Thus, sites with low productivity like, BD and EW where we assigned summer peaks ( $\text{GPP} < 0.10 \text{ g O}_2 \text{ m}^{-2} \text{ day}^{-1}$ ) could also be considered relatively constant like T1. Nevertheless, the summer peak patterns for BD and EW are more evident than that of T1. Despite the low estimates of BD, EW and T1, our estimates are consistent with those of other rivers in the western United States (Hall and Tank 2003; Marcarelli et al. 2010; Benjamin et al. 2016).

While our statistical results did not point to a strong influence of nutrients on GPP, nutrient recycling is complex, and rates may be influenced by the algal community found in the stream network (Kendrick and Huryn 2015). We observed *Didymosphenia geminata* (didymo), an invasive alga in cold, oligotrophic conditions, in over half of the stream sites. The semi-labile nature of the didymo stalks (Aboal et al. 2012) may affect the availability of labile carbon for bacterial consumption (Bothwell et al. 2014). Labile carbon is readily available at the time scale of hours to days whereas semi-labile carbon turnover is at the scale of weeks or months (Piontek et al. 2011). Semi-labile organic matter is consumed more efficiently in areas with low nutrient concentrations (Romaní and Sabater 2000) and by heterotrophic bacteria, when labile compounds are not sufficient to meet the bacterial carbon and energy requirements (Piontek et al. 2011).

In addition, we acknowledge that trophic (e.g. grazing) and non-trophic (e.g. nutrient excretion and bed scour associated with spawning salmon) biotic interactions could have been an important factor responsible for some of the GPP and ER patterns observed (McIntyre et al. 2008; Griffiths and Hill 2014). For instance, top-down grazing by aquatic macroinvertebrates can alter periphyton growth and community composition (Rosemond 1994; Wellnitz and Rader 2003). Previous research from the Methow has also shown that spawning salmon can increase GPP during and shortly

following spawning (Benjamin et al. 2016). More specifically, low densities of spawning salmon in the Methow River have been shown to increase GPP by 46% during spawning (Benjamin et al. 2016), and model simulations suggest that these effects are likely to vary across river networks as local geomorphology and nutrient status shift (Bellmore et al. 2014).

Similar intra-annual patterns of GPP and ER may be expected in winter because ice cover is likely to occur every year at the sites where it was observed. However, as climate changes due to warming, ice cover may not be as prevalent. Additionally, most of the sites have a high relative bed stability so flows higher than average, as those during our study, but lower than bankfull discharge in the summer and fall should not influence stream metabolism substantially because it will not mobilize the streambed.

Finally, other studies have shown that metabolism is also variable at smaller and larger spatial (Finlay 2011; Yates et al. 2013; Bernhardt et al. 2017; Dodds et al. 2018) and temporal scales (Uehlinger and Naegeli 1998; Roberts et al. 2007; Beaulieu et al. 2013). The metabolic profiles of rivers may be fractal in nature in that metabolic heterogeneity observed at coarse temporal resolution and broad spatial extent is likely to be matched by heterogeneity at finer temporal and spatial scales—albeit the controls on metabolism are likely to be different at each scale. This pattern of nested heterogeneity has emerged from the recent expansion of water temperature monitoring in river networks (Steel et al. 2017), and as dissolved oxygen loggers become more affordable and reliable, the same patterns may be found for metabolism.

## Implications

Our findings emphasize the idea that ecological systems are scale dependent (sensu Levin 1992). Stream networks are heterogeneous patches that interact hierarchically, and we show that this heterogeneity can provide a template for asynchronous patterns of ecosystem function, such as stream metabolism. In turn, these patterns are likely to influence food web dynamics and the capacity for river systems to deliver desired goods and services, such as fish production. For instance, peaks in upstream production may subsidize downstream reaches during times of lower productivity via transport of biologically available organic matter and nutrients (Bellmore and Baxter 2014; Hotchkiss and Hall 2015). Quantifying spatial heterogeneity in ecosystem metabolism, as we have done here, combined with concurrent measurements of consumer data can lead to new insights in our understanding of energy flows in aquatic systems (Bernhardt et al. 2017). It also illuminates yet another component of

ecological heterogeneity that may be compromised by the ongoing homogenization of natural landscapes (Moore et al. 2010).

**Acknowledgements** The research was supported by the US Bureau of Reclamation Cooperative Agreement to Dr. A. Fremier at the University of Idaho and Washington State University, Project Numbers # R11AC17061 and # R15AC00005. Eric Berntsen helped with the daily discharge estimates. This paper was improved with critical reviews by Dr. Colden Baxter (Idaho State University), Dr. Chris Caudill (University of Idaho), and members of the Fremier Lab (Washington State University). Any use of trade, product, or firm names is for descriptive purposes only and does not imply endorsement by the U.S. Government.

## Compliance with ethical standards

**Conflict of interest** The authors declare that they have no conflict of interest.

## References

- Aboal M, Marco S, Chaves E, Mulero I, García-Ayala A (2012) Ultrastructure and function of stalks of the diatom *Didymosphenia geminata*. *Hydrobiologia* 695:17–24
- APHA (2005) Standard methods for the examination of water and wastewater, 21st edn. American Public Health Association, Washington, DC
- Aristegi L, Izagirre O, Elozegi A (2009) Comparison of several methods to calculate reaeration in streams, and their effects on estimation of metabolism. *Hydrobiologia* 635:113–124
- Bartoń K (2015) MuMIn: multi-model inference. R package version 1.15.1
- Beaulieu JJ, Arango CP, Balz DA, Shuster WD (2013) Continuous monitoring reveals multiple controls on ecosystem metabolism in a suburban stream. *Freshw Biol* 58:918–937
- Bellmore JR, Baxter CV (2014) Effects of geomorphic process domains on river ecosystems: a comparison of floodplain and confined valley segments. *River Res Appl* 30:617–630
- Bellmore JR, Fremier AK, Mejia F, Newsom M (2014) The response of stream periphyton to Pacific salmon: using a model to understand the role of environmental context. *Freshw Biol* 59:1437–1451. <https://doi.org/10.1111/fwb.12356>
- Benjamin JR, Bellmore JR, Watson GA (2016) Response of ecosystem metabolism to low densities of spawning Chinook Salmon. *Freshw Sci* 35:810–825
- Bergey EA, Getty GM (2006) A review of methods for measuring the surface area of stream substrates. *Hydrobiologia* 556:7–16
- Bernhardt ES, Heffernan JB, Grimm NB, Stanley EH, Harvey JW, Arroita M, Appling AP, Cohen MJ, McDowell WH, Hall RO, Read JS, Roberts BJ, Stets EG, Yackulic CB (2017) The metabolic regimes of flowing waters. *Limnol Oceanogr* 63:S99–S118. <https://doi.org/10.1002/lno.10726>
- Bernot MJ, Sobota DJ, Hall RO, Mulholland PJ, Dodds WK, Webster JR, Tank JL, Ashkenas LR, Cooper LW, Dahm CN, Gregory SV, Grimm NB, Hamilton SK, Johnson SL, McDowell WH, Meyer JL, Peterson B, Poole GC, Valett HM, Arango C, Beaulieu JJ, Burgin AJ, Crenshaw C, Helton AM, Johnson L, Merriam J, Niederlehner BR, O'Brien JM, Potter JD, Sheibley RW, Thomas SM, Wilson K (2010) Inter-regional comparison of land-use effects on stream metabolism. *Freshw Biol* 55:1874–1890
- Biedenharn DS, Copeland RR, Thorne CR, Soar PJ, Hey RD, Watson CC (2000) Effective discharge calculation: a practical guide. Technical Rep. No. ERDC/CHL TR-00-15, U.S. Army Corps of Engineers, Washington, D.C. 48 pp
- Bothwell ML, Taylor BW, Kilroy C (2014) The Didymo story: the role of low dissolved phosphorus in the formation of *Didymosphenia geminata* blooms. *Diatom res* 29:229–236
- Demars BOL, Thompson J, Manson JR (2015) Stream metabolism and the open diel oxygen method: principles, practice and perspectives. *Limnol Oceanogr Meth* 13:356–374
- Dodds WK, Higgs SA, Spangler MJ, Guinnip J, Scott JD, Hedden SC, Frenette BD, Taylor R, Schechner AE, Hoeninghaus DJ, Evans-White MA (2018) Spatial heterogeneity and controls of ecosystem metabolism in a Great Plains river network. *Hydrobiologia* 1:85–102
- Ensign SH, Doyle MW (2006) Nutrient spiraling in streams and river networks. *J Geophys Res Biogeosci* 111:1–13
- Finlay JC (2011) Stream size and human influences on ecosystem production in river networks. *Ecosphere* 2:art87. <https://doi.org/10.1890/ES11-00071.1>
- Finlay JC, Hood JM, Limm MP, Power ME, Schade JD, Welter JR (2011) Light-mediated thresholds in stream-water nutrient composition in a river network. *Ecology* 92:140–150
- Gordon ND, McMahon TA, Finlayson BL, Gippel CJ, Nathan RJ (2004) Stream hydrology: an introduction for ecologists, 2nd edn. Wiley, Chichester, England, p 429 (ISBN: 978-0-470-84358-1)
- Grace MR, Imberger SJ (2006) Stream metabolism: Performing & interpreting measurements. Water Studies Centre Monash University, Murray Darling Basin Commission and New South Wales Department of Environment and Climate Change
- Grace MR, Giling DP, Hladyz S, Caron V, Thompson RM, McNally R (2015) Fast processing of diel oxygen curves: estimating stream metabolism with BASE (Bayesian Single-station Estimation). *Limnol Oceanogr-Meth* 13:103–114
- Greenwood JL, Rosemond AD (2005) Periphyton response to long-term nutrient enrichment in a shaded headwater stream. *Can J Fish Aquat Sci* 62:2033–2045
- Griffiths NA, Hill WR (2014) Temporal variation in the importance of a dominant consumer to stream nutrient cycling. *Ecosystems* 17:1169–1185
- Griffiths NA, Tank JL, Royer TV, Roley SS., Rosi-Marshall EJ, Whiles MR, Beaulieu JJ, Johnson LT (2013) Agricultural land use alters the seasonality and magnitude of stream metabolism. *Limnol Oceanogr*. <https://doi.org/10.4319/lno.2013.58.4.1513>
- Hall RO, Hotchkiss ER (2017) Stream metabolism. In: Hauer FR, Lamberti GA (eds) *Methods in stream ecology*, volume 2, 3rd edn. Academic Press, Cambridge, pp 219–233
- Hall RO, Tank JL (2003) Ecosystem metabolism controls nitrogen uptake in streams in the Grand Teton National Park, Wyoming. *Limnol Oceanogr* 48:1120–1128
- Hall RO, Kennedy TA, Rosi-Marshall EJ (2012) Air–water oxygen exchange in a large, whitewater river. *Limnol Oceanogr Fluids Environ* 2:1–11. <https://doi.org/10.1215/21573689-1572535>
- Hall RO, Tank JL, Baker MA, Rosi-Marshall EJ, Hotchkiss ER (2016) Metabolism, gas exchange, and carbon spiraling in rivers. *Ecosystems* 19:73–86
- Hart AM (2013) Seasonal variation in whole stream metabolism across varying land use types. Masters thesis. Virginia Polytechnic Institute and State University. Blacksburg, Virginia, USA
- Hoellein TJ, Bruesewitz DA, Richardson DC (2013) Revisiting Odum (1956): a synthesis of aquatic ecosystem metabolism. *Limnol Oceanogr* 58:2089–2100
- Hotchkiss ER, Hall RO Jr (2015) Whole-stream <sup>13</sup>C tracer addition reveals distinct fates of newly fixed carbon. *Ecology* 96:403–416
- Izaguirre O, Agirre U, Bermejo M, Pozo J, Elozegi A (2008) Environmental controls of whole-stream metabolism identified from continuous monitoring of Basque streams. *J N Am Benthol Soc* 27:252–268



- Julian JP, Doyle MW, Stanley EH (2008) Empirical modeling of light availability in rivers. *J Geophys Res* 113:G03022. <https://doi.org/10.1029/2007JG000601>
- Kendrick MR, Hurn AD (2015) Discharge, legacy effects and nutrient availability as determinants of temporal patterns in biofilm metabolism and accrual in an arctic river. *Freshw Biol* 60:2323–2336
- Konrad CP (2006) Location and timing of river-aquifer exchanges in six tributaries to the Columbia River in the Pacific Northwest of the United States. *J Hydrol* 329:444–470
- Lamberti GA, Steinman AD (1997) A comparison of primary production in stream ecosystems. *J N Am Benthol Soc* 16:95–103
- Leopold LB (1994) *A view of the river*. Harvard University Press, Cambridge
- Levin SA (1992) The problem of pattern and scale in ecology. *Ecology* 73:1943–1967
- Marcarelli AM, Van Kirk RW, Baxter CV (2010) Predicting effects of hydrologic alteration and climate change on ecosystem metabolism in a western U.S. river. *Ecol Appl* 20:2081–2088
- McCutchan JH, Lewis WM, Saunders JF, Saunders (1998) Uncertainty in the estimation of stream metabolism form open-channel oxygen concentrations. *J N Am Benthol Soc* 17:155–164
- McIntyre PB, Flecker AS, Vanni MJ, Hood JM, Taylor BW, Thomas SA (2008) Fish distributions and nutrient cycling in streams: can fish create biogeochemical hotspots. *Ecology* 89:2335–2346
- Minshall GW, Shafiq B, Price WJ, Holderman C, Anders PJ, Lester G, Barrett P (2014) Effects of nutrient replacement on benthic macroinvertebrates in an ultraoligotrophic reach of the Kootenai River, 2003–2010. *Freshw Sci* 33:1009–1023
- Moore JW, McClure M, Rogers LA, Schindler DE (2010) Synchronization and portfolio performance of threatened salmon. *Conserv Lett* 3:340–348
- Moore J, Beakes MP, Nesbitt HK, Yeakel JD, Patterson DA, Thompson LA, Phillis CC, Braun DC, Favaro C, Scott D, Carr-Harris C, Atlas WI (2015) Emergent stability in a large, free-flowing watershed. *Ecology* 96:340–347
- Odum HT (1956) Primary production in flowing waters. *Limnol Oceanogr* 1:102–117
- Ogdahl ME, Loughheed VL, Stevenson RJ, Steiman AD (2010) Influences of multi-scale habitat on metabolism in a coastal Great Lakes watershed. *Ecosystems* 13:222–238
- Pinheiro JC, Bates DM, DebRoy S, Sarkar DR Core Team (2017) nlme: linear and nonlinear mixed effects models\_R package version 3.1–131
- Piontek J, Händel N, De Bodt C, Harlay J, Chou L, Engel A (2011) The utilization of polysaccharides by heterotrophic bacterioplankton in the Bay of Biscay (North Atlantic Ocean). *J Plankton Res* 33:1719–1735
- R Development Core Team (2013) R: a language and environment for statistical computing. R Foundation for Statistical Computing, Vienna, Austria. R 2.15.2 GUI
- Roberts BJ, Mulholland PJ, Hill WR (2007) Multiple scales of temporal variability in ecosystem metabolism rates: results from 2 years of continuous monitoring in a forested headwater stream. *Ecosystems* 10:588–606
- Román AM, Sabater S (2000) Variability of heterotrophic activity in Mediterranean stream biofilms: a multivariate analysis of physical-chemical and biological factors. *Aquat Sci* 62:205–215
- Rosemond AD (1994) Multiple factors limit seasonal variation in periphyton in a forest stream. *J N Am Benthol Soc* 13:333–344
- Saunders WC, Bouwes N, McHugh P, Jordan CE (2018) A network model for primary production highlights linkages between salmonid populations and autochthonous resources. *Ecosphere* 9:e02131. <https://doi.org/10.1002/ecs2.2131>
- Schindler DE, Armstrong JB, Reed TE (2015) The portfolio concept in ecology and evolution. *Front Ecol Environ* 13:257–263
- Song C, Dodds WK, Trentman MT, Ruegg J, Ford B (2016) Methods of approximation influence aquatic ecosystem, metabolism estimates. *Limnol Oceanogr-Meth* 14:557–569
- Steel EA, Beechie TJ, Torgersen CE, Fullerton AH (2017) Envisioning, quantifying, and managing thermal regimes on river networks. *Bioscience* 67:506–522
- Tank J, Rosi-Marshall E, Griffiths NA, Entekin SA, Stephen ML (2010) A review of allochthonous organic matter dynamics and metabolism in streams. *J N Am Benthol Soc* 29:118–146
- Townsend SA, Webster IT, Schult JH (2011) Metabolism in a groundwater-fed river system in the Australian wet/dry tropics: tight coupling of photosynthesis and respiration. *J N Am Benthol Soc* 30:603–620
- Uehlinger U (2006) Annual cycle and inter-annual variability of gross primary production and ecosystem respiration in a floodprone river during a 15-year period. *Freshw Biol* 51:938–950
- Uehlinger U, Naegeli MW (1998) Ecosystem metabolism, disturbance, and stability in a prealpine gravel bed river. *J N Am Benthol Soc* 17:165–178
- Ulseth AJ, Bertuzzo E, Singer GA et al (2018) Climate-induced changes in spring snowmelt impact ecosystem metabolism and carbon fluxes in an alpine stream network. *Ecosystems* 21: 373–390 <https://doi.org/10.1007/s10021-017-0155-7>
- Val J, Chinarro D, Pino MR, Navarro E (2016) Global change impacts on river ecosystems: a high-resolution watershed study of Ebro river metabolism. *Sci Tot Environ* 570:774–783
- Valett HM, Thomas SA, Mulholland PJ, Webster JR, Dahm CN, Fellows CS, Crenshaw CL, Peterson CG (2008) Endogenous and exogenous control of ecosystem function: N cycling in headwater streams. *Ecology* 89:3515–3527
- Venkiteswaran JJ, Schiff SL, Taylor WD (2015) Linking aquatic metabolism, gas exchange, and hypoxia to impacts along the 300-km Grand River, Canada. *Freshw Sci* 34:1216–1232
- Walter JA, Sheppard LW, Anderson TL, Kastens JH, Bjornstad ON, Liebhold AM, Reuman DC (2017) The geography of asynchrony. *Ecol Lett* 20:801–814
- Wellnitz T, Rader RB (2003) Mechanisms influencing community composition and succession in mountain stream periphyton: interactions between scouring history, grazing, and irradiance. *J N Am Benthol Soc* 22:528–541
- Wetzel RG (2001) *Limnology: lake and river ecosystems*. Academic Press, San Diego
- Yates AG, Brua RB, Culp JM, Chambers PA (2013) Multi-scaled drivers of rural prairie stream metabolism along human activity gradients. *Freshw Biol* 58:675–689
- Young RG, Hurn AD (1996) Interannual variation in discharge controls ecosystem metabolism along a grassland river continuum. *Can J Fish Aquat Sci* 53:2199–2211
- Zuckerman A (2015) Seasonal variation in empirical and modeled periphyton at the watershed scale. Masters thesis. University of Idaho, Moscow, Idaho, USA
- Zuur AF, Ieno EN, Walker N, Saveliev AA, Smith GM (2009) *Mixed effects models and extensions in ecology with R*. Springer, New York